

*Tellus* (2002), 54B, 462–475  
Printed in UK. All rights reserved

Copyright © Blackwell Munksgaard, 2002

TELLUS  
ISSN 0280–6509

## Observations of atmospheric variability and soil exhalation rate of radon-222 at a Russian forest site

### Technical approach and deployment for boundary layer studies

By I. LEVIN<sup>1\*</sup>, M. BORN<sup>1,2</sup>, M. CUNTZ<sup>1</sup>, U. LANGENDÖRFER<sup>1</sup>, S. MANTSCH<sup>1</sup>, T. NAEGLER<sup>1</sup>, M. SCHMIDT<sup>1</sup>, A. VARLAGIN<sup>3</sup>, S. VERCLAS<sup>1</sup> and D. WAGENBACH<sup>1</sup>, <sup>1</sup>*Institut für Umweltphysik, Universität Heidelberg, Im Neuenheimer Feld 229, 69120 Heidelberg, Germany;* <sup>2</sup>*Fachbereich Physik, Universität Marburg, Renthof 5, 35037 Marburg, Germany;* <sup>3</sup>*Svertsov Institute for Evolutionary and Ecological Problems, Leninskii pr. 33, 117071 Moscow, Russia*

(Manuscript received 9 July 2001; in final form 22 April 2002)

#### ABSTRACT

A monitor for continuous observations of the atmospheric <sup>222</sup>Rn daughter activity has been improved and successfully implemented in a field study in the European Taiga (Fyodorovskoye Forest Reserve). The  $\alpha$ -activity of the short-lived <sup>222</sup>Rn and <sup>220</sup>Rn (<sup>212</sup>Pb) decay products, which are attached to aerosols, is accumulated on a quartz aerosol filter and assayed on line by  $\alpha$ -spectroscopy. The  $\alpha$ -activity from the <sup>212</sup>Pb daughters is determined by spectroscopy and corrected for. This monitor is suitable to measure <sup>222</sup>Rn activities at hourly resolution down to 0.5 Bq m<sup>-3</sup> with an uncertainty well below  $\pm 20\%$ . The prototype of this monitor is run in Heidelberg on the roof of the Institute's building about 20 m above ground. For this site, the atmospheric radioactive disequilibrium was determined between the <sup>222</sup>Rn daughter <sup>214</sup>Po and <sup>222</sup>Rn, which has to be known in order to derive the atmospheric <sup>222</sup>Rn activity with the static filter method. We derived a mean disequilibrium <sup>214</sup>Po/<sup>222</sup>Rn = 0.704  $\pm$  0.081 for various meteorological conditions through parallel <sup>222</sup>Rn gas measurements with a slow pulse ionisation chamber. At the Russian field site, continuous activity observations were performed from July 1998 until July 2000 with half a year's interruption in summer/fall 1999. During intensive campaigns, a second monitor was installed at Fyodorovskoye at 15.6 m (July/August 1998), and at 1.8 m (July/August 1999 and October 1999) above ground. As expected, pronounced diurnal cycles of the <sup>222</sup>Rn daughter activity were observed at all sites, particularly during summer when the vertical mixing conditions in the atmospheric surface layer vary strongly between day and night. The lower envelope of the continuous measurements at Fyodorovskoye and at Heidelberg changes on synoptic timescales by a factor of 4–10 due to long-range transport changes between continental to more maritime situations. Generally, the <sup>222</sup>Rn activity at 26.3 m height at Fyodorovskoye is lower by a factor of 2–3 compared to Heidelberg at 20 m above ground. This unexpected result is due to considerably lower <sup>222</sup>Rn exhalation rates from the soils measured in the footprint of the Fyodorovskoye Forest tower compared to Heidelberg. With the inverted chamber technique <sup>222</sup>Rn exhalation rates in the range 3.3–7.9 Bq m<sup>-2</sup> h<sup>-1</sup> were determined at Fyodorovskoye for summer 1998 and autumn 1999 (wet conditions with water table depths between 5 and 70 cm). Only during the very dry summer of 1999 the mean <sup>222</sup>Rn exhalation rate increased by about a factor of five. All measured exhalation rates at the Fyodorovskoye Forest are considerably smaller by a factor of 2–10 compared to observations in the vicinity of Heidelberg (ca. 50–60 Bq m<sup>-2</sup> h<sup>-1</sup>) and generally in Western Europe.

\*Corresponding author.  
e-mail: [ingeborg.levin@iup.uni-heidelberg.de](mailto:ingeborg.levin@iup.uni-heidelberg.de)

## 1. Introduction

Uranium-238 is a trace component of all soils and the primary isotope in the main uranium–radium decay series. Radon-222, which is produced through  $\alpha$ -decay of radium-226 in the soil, is the only gaseous decay product in this series. As a noble gas, part of the  $^{222}\text{Rn}$  emanates from the soil grains into the soil air and diffuses to the atmosphere. Here it is left to atmospheric dilution and radioactive decay ( $T_{1/2} = 3.8$  d). As the  $^{226}\text{Ra}$  activity is rather constant in different soil types ( $10^{-2}$ – $10^{-1}$  Bq g $^{-1}$  soil), and the emanation coefficient as well as the diffusion constants in the soil air do not vary by orders of magnitude,  $^{222}\text{Rn}$  exhalation rates from continental soil surfaces are rather homogeneous (Dörr and Münnich, 1990). They vary between 20 and 100 Bq  $^{222}\text{Rn}$  m $^{-2}$  h $^{-1}$ , depending mainly on the grain size distribution of the soil material, soil porosity and soil humidity (Schery et al., 1984; Nazaroff, 1992; Schüßler, 1996). Compared to the continents, the  $^{222}\text{Rn}$  emanation from ocean surfaces is negligible (Wilkening and Clements, 1975). Therefore, the  $^{222}\text{Rn}$  activity of an air mass can be used as an indicator for its residence time over the continent. Moreover, on the regional scale,  $^{222}\text{Rn}$  can be used as a quantitative tracer to parameterise diurnal changes of the inversion layer depth. In comparison to other gases, such as carbon dioxide or methane, also exhaling out of the soil or emitted at the soil surface, it is possible to use  $^{222}\text{Rn}$  for source strength estimates of those other gases if the  $^{222}\text{Rn}$  flux at the soil surface is measured in addition (e.g. Dörr et al., 1983; Levin, 1984; Levin et al., 1989; Wilson et al., 1997; Kuhlmann et al., 1998; Biraud et al., 2000). The prototype of the  $^{222}\text{Rn}$  monitor described here was set up in Heidelberg on the roof of our Institute's building (Verclas, 1994; Cuntz, 1997). Here it was used for regional CH $_4$  and N $_2$ O emission estimates (Levin et al., 1999; Schmidt et al., 2001).

During the EUROSIBERIAN CARBONFLUX project, an improved version of this monitor was installed in Russia at a field measurement site in the Fyodorovskoye Forest Reserve (33°E, 56°N, about 300 km north-west of Moscow) in July 1998, and was run there with some interruptions until July 2000. Our purpose was to apply the so-called radon tracer method and estimate night-time CO $_2$  fluxes from the forest area using concurrent  $^{222}\text{Rn}$  and CO $_2$  observations, together with direct measurements of the  $^{222}\text{Rn}$  exhalation rate from soils in the footprint of this site. In addition, during three roughly weekly intensive campaigns, atmospheric  $^{222}\text{Rn}$  measurements were performed in the

forest at two levels to derive activity gradients within the canopy. These atmospheric profile data allow estimates of the vertical exchange coefficient in a simple box-model approach (Langendörfer et al., 2002). Moreover the continuous atmospheric  $^{222}\text{Rn}$  data are used for validation of mesoscale atmospheric transport model estimates (Chevallard et al., 2002).

The purposes of this paper are (1) to describe in detail the technical set-up of our improved  $^{222}\text{Rn}$  monitor and to document its analytical performance, and (2) to present the continuous measurements at the Fyodorovskoye forest site in comparison with the Heidelberg  $^{222}\text{Rn}$  data. In addition, the results of the measured  $^{222}\text{Rn}$  exhalation rates in the footprint of the Fyodorovskoye tower are presented and discussed in relation to the respective hydrological situation.

## 2. Sampling and measurement techniques

### 2.1. Atmospheric $^{222}\text{Rn}$ activity

*2.1.1. Measurement principle.* The short-lived daughters of  $^{222}\text{Rn}$ , namely  $^{218}\text{Po}$  ( $T_{1/2} = 3$  min) and  $^{214}\text{Po}$  ( $T_{1/2} = 162$   $\mu\text{s}$ ) are metals, and, therefore, immediately after generation they become attached to sub-micron aerosol particles. Depending on the meteorological conditions, and the distance from the earth's surface, the  $^{222}\text{Rn}$  daughters are close to radioactive equilibrium with atmospheric  $^{222}\text{Rn}$ . Hence, provided the disequilibrium is known, the atmospheric  $^{222}\text{Rn}$  (gas) activity can be determined via its short-lived daughter activity. Based on earlier work by Volpp (1984), we developed an improved version of a  $^{222}\text{Rn}$  monitor using the static filter method. This consists of a specially designed filter holder with  $\alpha$ -detector and pre-amplifier as well as dedicated analogue and digital electronics. Ambient air is continuously pumped through a quartz filter. The  $^{222}\text{Rn}$  (and  $^{220}\text{Rn}$ , see below) daughters which are attached to aerosols are quantitatively collected on the filter. The  $\alpha$ -decay of the  $^{222}\text{Rn}$  daughters,  $^{218}\text{Po}$  ( $\alpha_E = 6.0$  MeV) and  $^{214}\text{Po}$  ( $\alpha_E = 7.7$  MeV), is measured in situ with a surface barrier detector. The mean  $\alpha$ -activity of the  $^{222}\text{Rn}$  daughters measured during a certain time interval (e.g. half an hour) on the filter is proportional to the atmospheric  $^{222}\text{Rn}$  daughter activity approximately one hour before. This "time delay" is due to the pure  $\beta$ -emitters  $^{214}\text{Pb}$  and  $^{214}\text{Bi}$  having a half-life of 26.8 and 19.8 min,

respectively, thus leading to a time lag of the measured  $\alpha$ -activity ( $^{214}\text{Po}$ ) on the filter.

A principal shortcoming in determining the atmospheric  $^{222}\text{Rn}$  daughter activity accurately with the static filter technique is the interference of the  $\alpha$ -activity of the  $^{220}\text{Rn}$  daughters.  $^{220}\text{Rn}$  is the very short-lived ( $T_{1/2} = 55.6$  s) radon isotope of the  $^{232}\text{thorium}$  decay series and also produced in all soils. Its decay products,  $^{212}\text{Po}$  ( $\alpha_E = 8.8$  MeV), and  $^{212}\text{Bi}$  ( $\alpha_E = 6.1$  MeV), are also collected on the filter. We overcome this problem by resolving the composite spectrum of the  $\alpha$ -activity on the filter with sufficiently high energy resolution allowing one to separate the  $^{220}\text{Rn}$  daughter from the  $^{222}\text{Rn}$  daughter activity. The accumulated  $\alpha$ -counts of both  $^{222}\text{Rn}$  daughters,  $^{214}\text{Po}$  and  $^{218}\text{Po}$  can not, however, be separated. Thus radioactive equilibrium on the filter is assumed between  $^{214}\text{Po}$  and  $^{218}\text{Po}$ , and the respective  $^{218}\text{Po}$  counts (5.79%) are subtracted from the total  $^{222}\text{Rn}$  daughter counts on the filter. The  $^{214}\text{Po}$  activity on the filter, which is in radioactive equilibrium with the  $^{214}\text{Bi}$  activity on the filter, is then used to determine the atmospheric  $^{214}\text{Po}$  activity (which is in radioactive equilibrium with the atmospheric  $^{214}\text{Bi}$  activity), taking into account the flow rate through the filter, the filter efficiency and the solid angle of the  $\alpha$ -detector. A detailed description of the experimental set up, the theoretical filter equations and the final calculation of the atmospheric  $^{214}\text{Po}$  activity from the measured filter activity are given in the Appendix.

*2.1.2. Determination of the atmospheric  $^{222}\text{Rn}$  activity.* In our geophysical application, we are finally interested in the atmospheric  $^{222}\text{Rn}$  activity. It is possible to derive this quantity if the disequilibrium between  $^{222}\text{Rn}$  activity and the (measured) atmospheric  $^{214}\text{Po}$  activity in ambient air is known. This relationship mainly varies with the meteorological conditions, the height above ground and the number of aerosol particles determining the fraction of unattached Rn daughters (e.g. Jacobi and André, 1963; Whittlestone, 1990; Porstendörfer et al., 1991; Schery and Wasiolek, 1993). Deviations from radioactive equilibrium may occur also during strong aerosol scavenging events. For continental sites such as Heidelberg or Fyodorovskoye, lowest aerosol particle number concentrations are in the order of  $10^4$   $\text{cm}^{-3}$ , so that the fraction of unattached Rn daughters is probably only in the order of a few percent (Reineking and Porstendörfer, 1990). For our Heidelberg measurement site 20 m above ground in the suburbs of the city, the mean disequilibrium has been determined by par-

allel measurement of  $^{214}\text{Po}$  with the radon monitor and the  $^{222}\text{Rn}$  activity with a slow-pulse ionisation chamber (Fischer, 1976). For different seasons and different meteorological conditions, a mean disequilibrium factor  $^{214}\text{Po}/^{222}\text{Rn}$  of  $0.704 \pm 0.081$  ( $n = 17$ ) was found (Cuntz, 1997). A value of  $0.755 \pm 0.026$  ( $n = 8$ ) was determined for convective afternoon conditions only. When large short-term changes of the atmospheric  $^{222}\text{Rn}$  activity occur, as is the case during the build-up of strong night-time inversions, disequilibrium factors as small as 0.63 were observed. Our measurements of the  $^{214}\text{Po}/^{222}\text{Rn}$  disequilibrium are to be compared with results from Volpp (1984), who determined disequilibrium factors between 0.73 and 0.95 for the same Heidelberg measurement site (although at a height of 17.4 m above ground). Theoretical calculations made by Jacobi and André (1963) for 10 m above ground yield a mean disequilibrium of 0.835 ranging from 0.73 to 0.97, depending on the turbulent diffusion coefficient in the atmosphere. For 100 m above ground, Jacobi and André calculate a mean disequilibrium of 0.915 with a range of 0.88–1.0. More sophisticated model estimates by Schery and Wasiolek (1993) and their direct observations as well as observations by Porstendörfer et al. (1991), although at lower heights above ground, yield slightly lower values. From this comparison with earlier experimental data and theoretical calculations we conclude that our experimentally determined mean disequilibrium factor of  $0.704 \pm 0.081$  falls well within the range of other investigations.

However, the Heidelberg disequilibrium factor scales linearly with the calibration of the efficiency of our radon ionisation chambers. This calibration was originally performed in two ways: the efficiency of the chambers was calculated theoretically from their geometry and the comparison between a theoretical  $\alpha$ -spectrum with the actually measured spectrum. In this way the efficiency was calculated to 96% (Fischer, 1976). In addition, standard  $^{222}\text{Rn}$  samples derived from an absolutely calibrated radium-226 solution were injected into the chambers which yielded efficiencies between 92 and 94%. The efficiency of the chambers was thus estimated by Roether and Kromer (1978) to be “better than 95%”. The chambers had originally been designed and used for  $^{222}\text{Rn}$  analyses in surface ocean water to derive gas exchange rates. In later years, they were only used for soil radon investigations as in the present study. In their study of  $^{222}\text{Rn}$  exhalation rates from soils in West Germany, Dörr and Münnich (1990) assumed a counting efficiency of the

ionisation chambers of only 81%. This number was applied to all subsequent measurements, including the determination of the  $^{214}\text{Po}/^{222}\text{Rn}$  disequilibrium factor by Cuntz (1997).

In order to be comparable to these earlier studies, we used here the same value for the chamber efficiency as Dörr and Münnich (1990). However, one has to keep in mind that this value may be too low by up to 15%, and that the disequilibrium factors for the Heidelberg measurement site may also be underestimated by the same amount. In fact, a larger chamber efficiency would bring the disequilibrium factors up to the experimentally determined values of Volpp (1984) and to the theoretical calculations by Jacobi and André (1963). However, for the studies applying the radon tracer method (i.e. Levin et al., 1999; Langendörfer et al., 2002; Schmidt et al., 2001) the absolute value of the atmospheric  $^{222}\text{Rn}$  activity is not important, as long as the soil exhalation fluxes applied in these studies are determined with the same ionisation chamber efficiency as the atmospheric  $^{214}\text{Po}/^{222}\text{Rn}$  disequilibrium. Therefore, we applied a  $^{214}\text{Po}/^{222}\text{Rn}$  disequilibrium factor of  $0.704 \pm 0.081$  to all Heidelberg  $^{214}\text{Po}$  activities to derive atmospheric  $^{222}\text{Rn}$  gas activities. Although the disequilibrium has been observed and theoretically calculated to change with the meteorological situation and the aerosol concentration, we use here a constant value; the uncertainty associated with this simplification is in the order of  $\pm 10\%$ .

For the Fyodorovskoye measurement site, an experimental determination of disequilibrium factors was not possible. However, from the discussion above, for the upper measurement level (at 26.3 m above ground, and about 3 m above the forest canopy) it is fair to assume a disequilibrium factor close to the one measured in Heidelberg. For the low measurement levels (15.6 m in July 1998 and 1.8 m in July and October 1999), following the theoretical calculations by Jacobi and André (1963), the disequilibrium factors should be close to that at 26.3 m for daytime situations, whereas a significantly smaller factor should be valid at least for the 1.8 m level during stable night-time situations, particularly in summer. The mean theoretical disequilibrium factor for four different stability classes for 1 and 10 m above ground is calculated from Table 1 in Jacobi and André (1963) to be 0.745. This factor is about 17% higher than the mean theoretical value for 10 and 100 m above ground (i.e. 0.878). In order to take into account that the disequilibrium factor decreases from 26.3 to 1.8 m, at least during stable nights,

and to derive a consistent data set (in terms of absolute calibration of our records), as a first estimate we therefore used a disequilibrium factor for the summer 1999 campaign at 1.8 m of  $0.704/1.17 = 0.6$ .

When comparing our observations from the two measurement levels during the autumn 1999 campaign, the activity data in the two heights (when calculated assuming no disequilibrium, i.e. a disequilibrium factor of 1) do not show any significant gradient neither during the day nor during night. This finding may suggest a well mixed atmospheric surface layer and equal disequilibrium factors at both levels. The same is true for the summer 1998 campaign when comparing the 26.3 m and the 15.6 m levels. Therefore, we decided to apply one constant disequilibrium factor to all measurements performed at the respective two levels for summer 1998 and autumn 1999, namely  $0.704 \pm 0.081$  (the same value as for Heidelberg). This decision is supported by the finding that the influence of  $^{222}\text{Rn}$  exhalation in the immediate footprint of the measurement site during the summer 1998 and the autumn 1999 campaign was probably very small due to the very small exhalation rates. During the summer 1999 campaign the situation was different with soil exhalation rates larger by almost one order of magnitude, and a respectively larger contribution of  $^{222}\text{Rn}$  exhalation from the immediate footprint to the observed vertical gradient (Section 3.1).

*2.1.3. Discussion of the atmospheric  $^{222}\text{Rn}$  data quality.* The total uncertainty of the atmospheric  $^{222}\text{Rn}$  activity determined with the  $^{222}\text{Rn}$  monitor via the atmospheric daughter activity can be estimated for Heidelberg to  $\pm 17\%$ , which is mainly due to systematic errors of the disequilibrium between  $^{222}\text{Rn}$  and  $^{214}\text{Po}$  in the atmosphere and  $^{214}\text{Pb}$  and  $^{214}\text{Bi}$  on the filter both contributing about 10% (Cuntz, 1997). A comparably smaller uncertainty is associated with the statistical counting error (for half-hourly values, ca.  $\pm 4\%$ ) and the flow rate error (ca.  $\pm 4\%$ ). The field observations at Fyodorovskoye have a slightly larger uncertainty: due to constraints of the electrical power supply, the flow rate here was only about 60% of the flow rate in Heidelberg, and the measured activity was only 20–30% of that generally measured in Heidelberg. The statistical counting errors of the Fyodorovskoye measurements were therefore in the order of  $\pm 6\%$ . In addition, we were not able to determine the disequilibrium factors for the two measurement levels experimentally, so that the uncertainty of this parameter is probably here in the order of  $\pm 15\%$ . All these uncertainties lead to a total uncertainty of the

Fyodorovskoye  $^{222}\text{Rn}$  measurements of  $\pm(20\text{--}25)\%$ . Note that determination of relative  $^{222}\text{Rn}$  gradients is much more accurate, in the order of only  $\pm 15\%$ . This can be derived from the standard deviation of the gradient observed during the July 1998 campaign (Fig. 5a) which is in the order of only  $\pm(10\text{--}15)\%$ .

## 2.2. Procedures to measure $^{222}\text{Rn}$ exhalation rates at the soil surface

### 2.2.1. Sampling procedure for soil exhalation samples.

Soil exhalation samples for  $^{222}\text{Rn}$  analyses have been collected with the closed chamber method following the procedure by Dörr and Münnich (1990). The basis part of a stainless steel chamber (0.6 m  $\times$  0.6 m, ca. 0.3 m high), an open frame, was driven about 3–5 cm into the soil and left there for about 10–20 min to adjust disturbances of the soil surface. Then the top was mounted on the frame and sealed with water. Immediately after closure of the chamber, a “start” sample was collected (this sample was only analysed for  $\text{CO}_2$  and  $\text{CH}_4$  concentration to provide a measure of the disturbance of the topsoil during installation of the chamber). The exhaling soil gases were then accumulated for about one hour, and a sample was subsequently collected. The long exposure time was necessary in this study to yield measurable  $^{222}\text{Rn}$  activities; however, through this constraint, all measured fluxes, including the  $^{222}\text{Rn}$  exhalation rate, may be underestimated due to possible back-diffusion of gases from the chamber air into the soil. Air samples from the chamber were collected into 500 mL aluminium-coated polyethylene bags using a gas-tight 50 mL syringe. The sample bags have been regularly tested to be gas-tight through duplicate measurements of their  $^{222}\text{Rn}$  activity on consecutive days. During the July 1998 sampling campaign, the water table depth was also measured at each sampling location.

### 2.2.2. $^{222}\text{Rn}$ activity determination of soil exhalation samples.

The soil exhalation samples were transported from the field site (Fyodorovskoye) to the laboratory in Heidelberg within 24 h, and an aliquot of about 100–200 mL was injected into the same slow-pulse ionisation chambers (Fischer, 1976) which were used for determination of the atmospheric disequilibrium factors between  $^{222}\text{Rn}$  and  $^{214}\text{Po}$  at the Heidelberg measurement site (Section 2.1.2). Typical counting rates of the exhalation samples were in the order of 0.5–5 cpm. Each sample was counted for about 12 h. Typical counting errors were in the order of  $\pm 5\%$ .  $^{222}\text{Rn}$  exhalation rates at the soil surface were deter-

mined assuming a linear concentration change under the chamber with the initial concentration set to the lowest level atmospheric observation. The typical error of a  $^{222}\text{Rn}$  flux determination is estimated to  $\pm 10\%$ .

## 3. Observational results

### 3.1. $^{222}\text{Rn}$ soil exhalation rates within the footprint of the Fyodorovskoye tower

During each of the intensive campaigns at the Fyodorovskoye field site, at least one transect of soil exhalation sampling has been performed. Samples were collected in the immediate neighbourhood of the meteorological tower (“Tower”), at two additional sites south (“Forest”) and east (“Bog”) of the tower close to a small bog as well as along a transect (Rn-1 to Rn-7) which is characterised by different water table depths and consequently different plant cover. In August 2000, an additional site, FTC, was sampled (4 positions in an area of about 50 m  $\times$  50 m), because it turned out that one rather frequent soil type had not been sampled in the footprint of the tower. A map of the sampling sites, including the location of the atmospheric observational tower, is shown in Fig. 1. The area of the footprint can be roughly separated into three different soil and vegetation types: Type A, immediately around the tower is poorly drained with water table depths between 5 and 15 cm below soil surface. A peat layer of about 50 cm thickness is covering

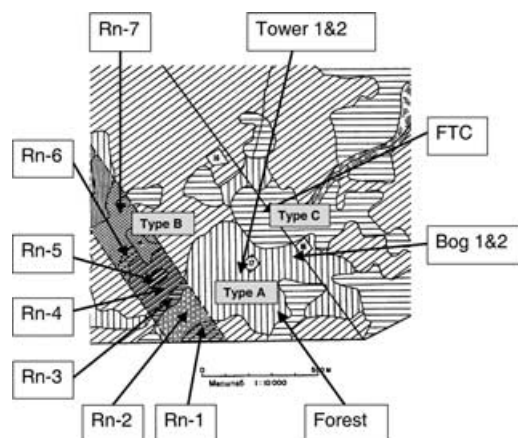


Fig. 1. Map of the  $^{222}\text{Rn}$  exhalation sampling sites around the Fyodorovskoye Forest Reserve tower located in the European Taiga ( $33^\circ\text{E}$ ,  $56^\circ\text{N}$ ; basic map courtesy of T. Minaeva).

the light-loamy soil underneath. Vegetation is mainly spruce with sphagnum mosses and blueberries as understory. On Type B the peat layer is generally missing; these areas are about 1–2 m higher in elevation than type A and are better drained. The vegetation consists of spruce and poplar with fern and raspberries as understory. Type C is intermediate between A and B with respect to its hydrological and vegetation conditions.

All individual results from the soil exhalation samples collected during the five “wet” and the two “dry” radon transects are presented in Figs. 2a and b. During wet conditions, mean exhalation rates from soil

type A ( $3.3 \pm 0.9 \text{ Bq m}^{-2} \text{ h}^{-1}$ ) are generally lower by a factor of two or more compared to type B ( $7.9 \pm 2.1 \text{ Bq m}^{-2} \text{ h}^{-1}$ ). This ratio changes little between the different transects. The mean exhalation rate from soil type C ( $3.6 \pm 1.3 \text{ Bq m}^{-2} \text{ h}^{-1}$ ) in August 2000 was in the range of exhalation rates from type A. Contrary to the normally “wet” situation in Fyodorovskoye, with a water table depth between 5 cm and about 70 cm in the footprint of the tower, summer 1999 (July and August) was extraordinary dry. A much deeper water table depth during this campaign manifests itself in a seven-fold higher <sup>222</sup>Rn exhalation rate from soil type

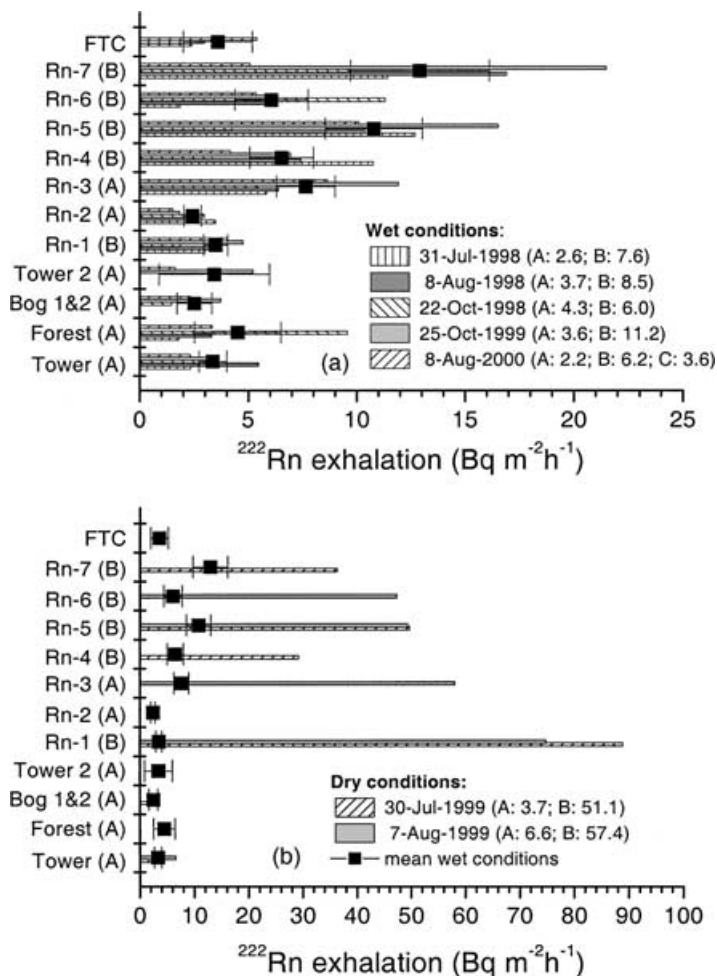


Fig. 2. (a) <sup>222</sup>Rn exhalation rates measured during normal “wet” conditions at the sampling sites of Fig. 1. The squares are the mean exhalation rates for all “wet” transects at the respective sites. (b) Same as (a) but for dry conditions during summer 1999 (note the different <sup>222</sup>Rn scales). The numbers given in the legends are the mean values in  $\text{Bq m}^{-2} \text{ h}^{-1}$  for soil types A, B and C, respectively, for the different transects.

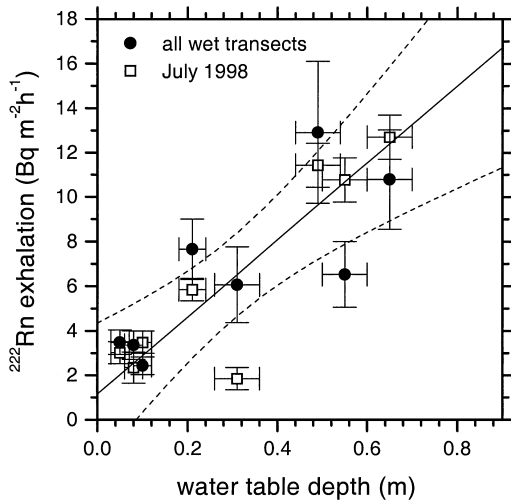


Fig. 3. Relation between  $^{222}\text{Rn}$  exhalation rates and water table depth. The solid line shows the linear regression calculated through the July 1998 data when water table depth was actually measured. Assuming that the water table depths are similar during all wet transects, the mean  $^{222}\text{Rn}$  exhalation rates (full circles) also follow this relation. Dashed lines give the lower and upper limits of the 95% confidence interval.

B ( $54.2 \pm 7.0 \text{ Bq m}^{-2} \text{ h}^{-1}$ ). The rates from soil type A ( $4.7 \pm 1.2 \text{ Bq m}^{-2} \text{ h}^{-1}$ ) were only about 50% higher than during wet conditions.

The strong relation between water table depth and  $^{222}\text{Rn}$  exhalation rate is also visible in Fig. 3. Here the  $^{222}\text{Rn}$  exhalation rates from the different sites sampled in July 1998 are plotted against the water table depth, which was roughly determined with a simple bubbling tube. As shown by Dörr and Münnich (1990), the theoretical  $^{222}\text{Rn}$  concentration profile  $c_{\text{Rn}}(z)$  in a soil with a homogeneous  $^{222}\text{Rn}$  emanation rate is described by a steady-state depth profile

$$c_{\text{Rn}}(z) = c_{\infty}[1 - \exp(-z/\bar{z})] \quad (1)$$

with the equilibrium concentration  $c_{\infty}$  observed at large depths. Depending on soil texture, the characteristic penetration depth  $\bar{z}$  was deduced as 0.3 m in very wet and fine-grained soils and about 1.7 m in sandy soils with water table depths well below several metres (Dörr and Münnich, 1990). The exhalation rate at the soil surface  $j_{\text{Rn}}(z=0)$  can be derived from the profile and from the permeability (molecular diffusion coefficient)  $P_{\text{Rn}}$  in the soil air as

$$j_{\text{Rn}}(z=0) = -P_{\text{Rn}} \frac{c_{\infty}}{\bar{z}}. \quad (2)$$

At our measurement sites where the water table depths were very shallow  $^{222}\text{Rn}$  saturation in the soil air was already reached at several centimetres, and the respective  $\bar{z}$ , and also the equilibrium concentration  $c_{\infty}$ , are very low. Moreover, the permeability  $P_{\text{Rn}}$  is small under high soil humidity, which all together lead to very small  $^{222}\text{Rn}$  exhalation rates. Only during summer 1999, when the water table at sampling sites of soil type B decreased to several metres below the surface, the respective  $\bar{z}$  and, therewith  $c_{\infty}$ , achieved "normal" values with  $^{222}\text{Rn}$  exhalation rates in the same order as observed by Dörr and Münnich (1990) at dry sites with sandy-loamy soil types in Western Europe.

### 3.2. Long-term $^{222}\text{Rn}$ activity observations at Fyodorovskoye from July 1998 to July 2000 in comparison to the Heidelberg measurements

The continuous record of  $^{222}\text{Rn}$  activities derived from  $^{214}\text{Po}$  measurements at the Fyodorovskoye field site at 26.3 m above ground is shown in Fig. 4a. During the second half of 1999, due to data acquisition problems observations are only available during the intensive campaigns in July and October (see also Figs. 5b and c). The atmospheric  $^{222}\text{Rn}$  activity at this forested site generally varies between 0.5 and  $10 \text{ Bq m}^{-3}$ . The lower envelope of the record changes on synoptic timescales (3–5 d) between 0.5 and about  $6 \text{ Bq m}^{-3}$ ; lowest activities are generally observed in spring and summer while the highest values are found from October to December. In the period from April until September, we generally observe regular diurnal cycles with mean peak-to-peak amplitudes of 2–3  $\text{Bq m}^{-3}$ . For comparison, Fig. 4b shows the continuous record of half-hourly atmospheric  $^{222}\text{Rn}$  activity data at the Heidelberg measurement site. Here the activity concentration is generally higher than at Fyodorovskoye and varies between 2 and  $30 \text{ Bq m}^{-3}$ , with large diurnal changes during the summer months. These diurnal changes are generally higher by a factor of 2–3 if compared to the Fyodorovskoye forest site. The minimum activities in Heidelberg vary between 2 and  $5 \text{ Bq m}^{-3}$  during the summer months. During autumn and winter we frequently observe longer-lasting episodes of  $^{222}\text{Rn}$ -enriched continental air masses with minimum activity levels as high as  $20 \text{ Bq m}^{-3}$ . The Heidelberg  $^{222}\text{Rn}$  record has already been used in several studies to estimate radon-derived fluxes of various trace gas

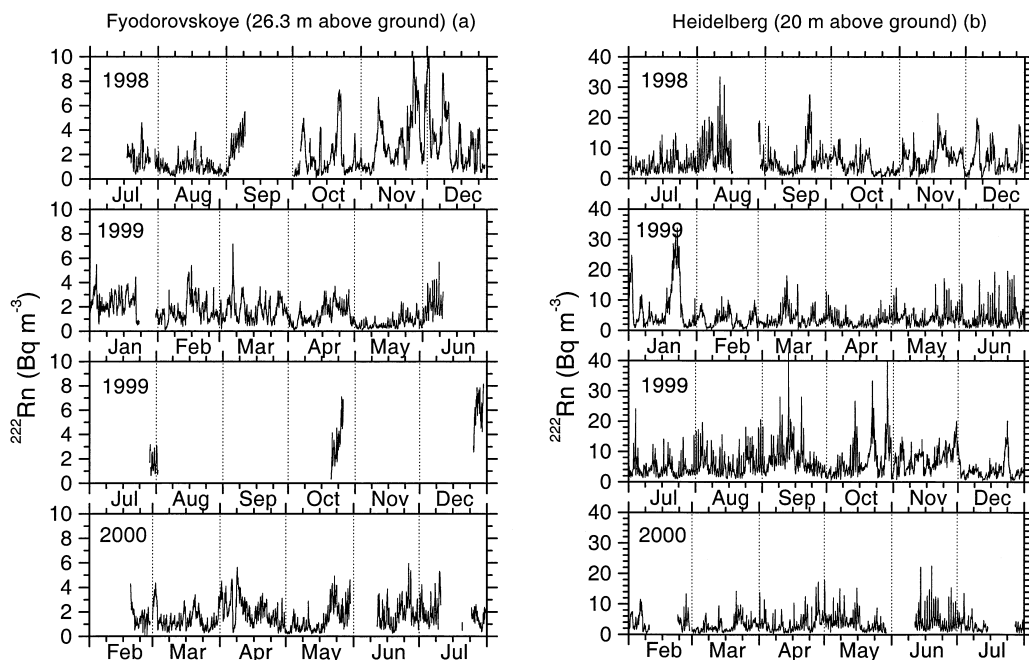


Fig. 4. (a) Atmospheric  $^{222}\text{Rn}$  activity observed at 26.3 m above ground at the Fyodorovskoye forest site. (b) Same as (a) but for Heidelberg at 20 m above ground. (Half-hourly data have been smoothed over three points to derive an effective time resolution of 1 h.)

emissions (Levin et al., 1989; 1999; Schmidt et al., 2001).

Summarising the comparison of atmospheric  $^{222}\text{Rn}$  activities between Fyodorovskoye and Heidelberg we can conclude that not only baseline activities but also the diurnal amplitudes in summer are generally higher in Heidelberg by a factor of 2–3 than at Fyodorovskoye. Qualitatively, this is not surprising if we compare the soil exhalation rates in the footprint of the two sites. While mean soil exhalation rates in the Heidelberg catchment area are in the order of  $50\text{--}60 \text{ Bq m}^{-2} \text{ h}^{-1}$ , they are only in the order of  $3\text{--}8 \text{ Bq m}^{-2} \text{ h}^{-1}$  in the footprint of Fyodorovskoye during most of the time (wet conditions, see Section 3.1). If, as a first-order approach, we can scale observed atmospheric activities with the ground-level fluxes in the respective footprints, a general concentration difference of almost one order of magnitude would be expected. The fact that Fyodorovskoye atmospheric activities are only lower by a factor of 2–3 compared to Heidelberg indicates a discrepancy by a factor of about 3–5 between direct emissions and atmospheric concentrations. Excluding systematic errors of this mag-

nitude in our atmospheric measurements but also in soil exhalation rates, this discrepancy can only be explained by an underestimation of the catchment area of the Fyodorovskoye tower. Obviously, the catchment area in reality is much larger than that shown in Fig. 1, and approximated by a radius of 1–2 km around the measurement site (Schuepp et al., 2000; Rebmann and Kolle, 2000). From an inspection of soil and vegetation types in the larger area around the measurement site (50–100 km radius, a distance which is accessible during half a day with a mean wind velocity of  $2 \text{ m s}^{-1}$ ), it is quite plausible that the  $^{222}\text{Rn}$  exhalation rates are considerably higher there, largely contributing to the general  $^{222}\text{Rn}$  activity level at the Fyodorovskoye measurement site.

### 3.3. $^{222}\text{Rn}$ activity observations at two heights during the summer and autumn field campaigns

During intensive field campaigns at Fyodorovskoye,  $^{222}\text{Rn}$  observations have been performed at two heights. At the start of the first campaign, at this new measurement tower no information about the



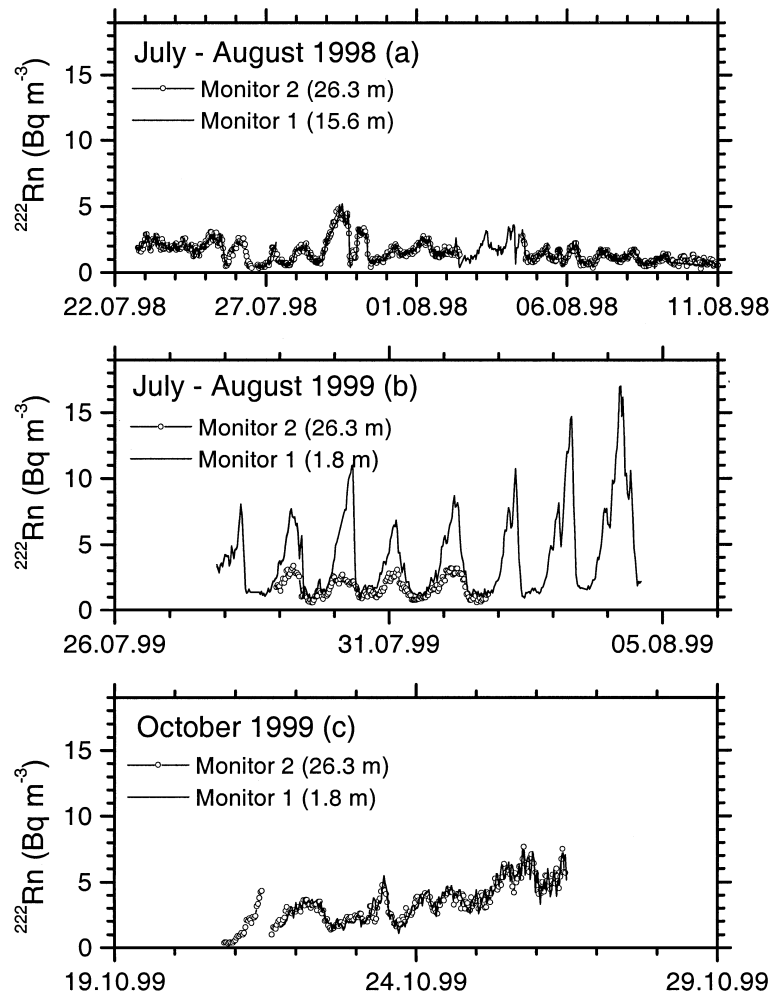


Fig. 5. (a) Atmospheric  $^{222}\text{Rn}$  activity observed at 26.3 and 15.6 m above ground during the July/August 1998 field campaign (smoothing as in Fig. 4). The data of the two heights are indistinguishable. (b) Atmospheric  $^{222}\text{Rn}$  activity observed at 26.3 and 1.8 m above ground during the July/August 1999 field campaign (smoothing as in Fig. 4). (c) Same as (b) but for the autumn field campaign in October 1999 (smoothing as in Fig. 4). Similar to the summer 1998 campaign, the data of the two heights are indistinguishable.

micrometeorological situation within the canopy of the forest had been available. Therefore, we chose as a second measurement level a height of 15.6 m above ground, the lower limit of the upper canopy level. Fig. 5a shows the measurements at the two levels. No significant gradient is observed between these two heights. This finding has the following consequences: (1) Obviously, during both day and night the upper part of the forest canopy is well mixed. (2) Concerning the unknown disequilibrium factor between  $^{222}\text{Rn}$  and

its daughters, the striking similarity between the two records suggests that the disequilibrium factor does not significantly differ between these two heights (see also Section 2.1.2).

For the summer and autumn 1999 field campaigns the second observational level was lowered to 1.8 m above ground. The  $^{222}\text{Rn}$  activities during these two campaigns are plotted in Figs. 5b and 5c. During the summer 1999 season we now observe very strong night-time gradients, but during daytime again the

gradients almost disappear. The conditions change again in the October 1999 field campaign when during day *and* night the gradient between 1.8 and 26.3 m disappears. There are two possible explanations for this unexpected behaviour in October 1999: (1) Despite a measurable  $^{222}\text{Rn}$  exhalation rate at the ground, due to strong vertical mixing no vertical gradient could be established, and (2) during wet conditions, the  $^{222}\text{Rn}$  exhalation rate in the immediate footprint of the tower can be neglected compared to the  $^{222}\text{Rn}$  emissions originating from a larger catchment area. Both explanations are in accordance with the results from the summer 1998 and summer 1999 campaigns. In summer 1998, the soil exhalation rate is similar to that in October 1999, and no vertical gradient is observed. In summer 1999, the  $^{222}\text{Rn}$  exhalation rates are larger by a factor of about 6–7 than during wet conditions, and a significant vertical gradient can be established, at least during the night.

#### 4. Conclusions

Atmospheric  $^{222}\text{Rn}$  monitoring based on continuous sampling and  $\alpha$ -counting of  $^{222}\text{Rn}$  and  $^{220}\text{Rn}$  decay products is shown (1) to give reliable results at hourly resolution with a typical uncertainty (including disequilibrium problems) of  $\pm 20\%$ , (2) to be well suited for field studies, dedicated to the budgeting of (long-lived) trace gases in boundary layer air. Application of the instrument at two regions, Fyodorovskoye in the European Taiga and Heidelberg in Germany, significantly differing with respect to soil type, hydrological conditions and plant cover, revealed that reliable and representative observation of the spatio-temporal pattern of the  $^{222}\text{Rn}$  exhalation rate is mandatory to an understanding of the observed atmospheric  $^{222}\text{Rn}$  activity levels. This is even more important if the data are to be used for mesoscale model validation (Chevallard et al., 2002) or to successfully apply the radon tracer method (Langendörfer, 2002). Our atmospheric  $^{222}\text{Rn}$  observations from Fyodorovskoye Forest reserve, in combination with measured soil exhalation rates in the immediate neighbourhood (“eddy correlation footprint”) of the measurement site, indicate that continuous concentration measurements, even if they are performed only at heights of 20–30 m above ground, probably have a catchment area or area of immediate influence of several ten to hundred kilometres. This is considerably larger than what is estimated with classical footprint models which have been developed, i.e., for eddy cor-

relation towers and associated micro-meteorological studies. These give footprint areas which are only in the order of several kilometres around the respective measurement site.

#### 5. Acknowledgements

Measurements at the Fyodorovskoye Forest site have been made possible with the logistic support from IPEE, Moscow (Prof. N. N. Vygodskaya), the Central Forest Reserve, Fyodorovskoye, and MPI for Biogeochemistry, Jena (Prof. E.-D. Schulze). We thank all field workers at Fyodorovskoye Forest Reserve for their very helpful support. T. Minaeva provided the original map of Fig. 1. Her expertise and advice in choosing suitable sites for  $^{222}\text{Rn}$  exhalation measurements is gratefully acknowledged. This project has been partially funded by the European Commission under contracts EV5V-0048 and ENV4-CT-97-0491.

#### 6. Appendix

##### 6.1. General description of the Radon Monitor set up

Figure 6 shows the schematics of the Heidelberg  $^{222}\text{Rn}$  monitor. At a flow rate of about  $0.5\text{--}1.5\text{ m}^3\text{ h}^{-1}$  ambient air is continuously pumped through a quartz fibre filter (Whatman QMA,  $\varnothing 47\text{ mm}$ ); the flow rate is monitored with a flow meter (MKS type 0258CC-50000GV,  $50\text{ L min}^{-1}$  or EL-FLOW F112AC-HAD-22-V). The  $^{222}\text{Rn}$  (and  $^{220}\text{Rn}$ ) daughters  $^{218}\text{Po}$  ( $\alpha_{\text{E}} = 6.0\text{ MeV}$ ) and  $^{214}\text{Po}$  ( $\alpha_{\text{E}} = 7.7\text{ MeV}$ ) collected on the filter are measured in situ with a surface barrier detector (Canberra CAM AB 900  $\text{mm}^2$  active surface, energy resolution  $50\text{ keV}$  at an  $\alpha$ -energy of  $5.486\text{ MeV}$ ). A pre-amplifier converts the detector pulses into amplified voltage signals which can then be transmitted via cable over distances of up to  $100\text{ m}$ . This allows physical separation of the filter head from the main electronic board, and thus relatively short tubing connections between filter holder and ambient air. The signal is further amplified and processed by dedicated analogue and digital electronics.

A typical  $\alpha$ -spectrum of the  $^{222}\text{Rn}$  and  $^{220}\text{Rn}$  daughters collected on the quartz filter within a  $1\text{ h}$  integration time is presented in Fig. 7. Due to various absorption mechanisms, the  $\alpha$ -spectrum is distorted to lower energies (low-energy tailing). Three maxima are clearly distinguishable in the spectrum,

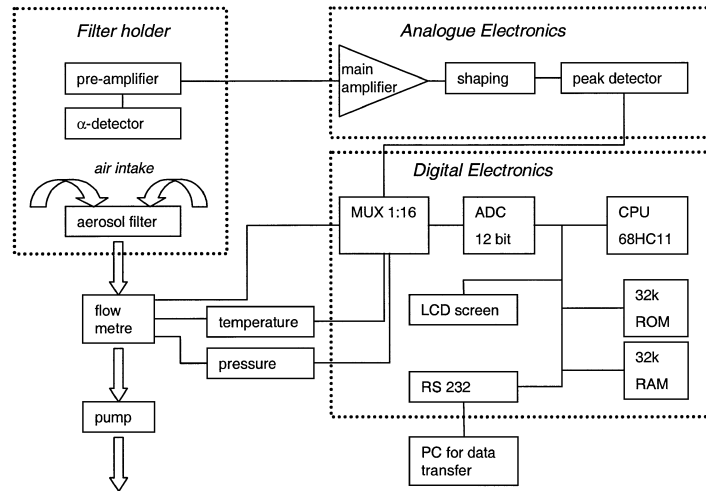


Fig. 6. Schematics of the Heidelberg radon monitor.

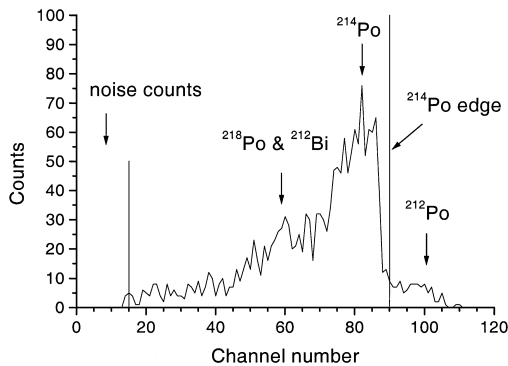


Fig. 7. Typical  $\alpha$ -spectrum of the  $^{222}\text{Rn}$  and  $^{220}\text{Rn}$  daughters collected in Heidelberg on a quartz glass filter with an integration time of 1 h. The different isotopes and the thresholds for evaluation of the spectrum are also marked on the diagram.

representing the  $\alpha$ -activity of  $^{212}\text{Po}$ ,  $^{214}\text{Po}$  and a mixture of  $^{218}\text{Po}$  and  $^{212}\text{Bi}$ . Depending on the time of day and the degree of filter loading, the ratio between the  $^{212}\text{Po}$  ( $^{220}\text{Rn}$  daughter) and  $^{214}\text{Po}$  ( $^{222}\text{Rn}$  daughter) may vary by nearly one order of magnitude. However, the  $^{220}\text{Rn}$ -derived  $^{212}\text{Po}$  peak can be easily resolved, and, hence separated from the  $^{214}\text{Po}$  peak, allowing for an accurate determination of the  $^{222}\text{Rn}$  daughter activity on the filter.

Overall technical data: Detection limit at 10% counting error with 1 h time resolution:  $0.2 \text{ Bq m}^{-3}$ . Power consumption: monitor without pump: 45–

50 mA at 230 V. Dimensions and weight: electronic rack:  $0.35 \times 0.30 \times 0.15 \text{ m}$ , 3 kg; filter head:  $0.1 \times 0.15 \times 0.2 \text{ m}$ , 1 kg.

## 6.2. Theoretical determination of the $^{214}\text{Po}$ activity $^{214}\text{Po}A_\alpha$ in the atmosphere from filter measurements $^{214}\text{Po}A_\alpha$

The temporal change of the radionuclide concentration  $^iN$  on a filter depends on its concentration  $^i n$  in the atmosphere and its deposition rate on the filter. It is described by a system of generalised Bateman equations (Schumann, 1956) ( $^{i-1}N$  is the daughter of radio nuclide  $^iN$ ):

$$\frac{d^iN}{dt} = \varepsilon Q^i n + {}^{i-1}N^{i-1}\lambda - {}^iN^i\lambda, \quad (\text{A1})$$

where  $\varepsilon$  is the filter efficiency,  $Q$  is the air flow rate ( $\text{m}^3 \text{ s}^{-1}$ ) through the filter, and  $^i\lambda$  are the decay constants of the individual radio nuclides  $i$ . The atmospheric concentration  $^i n$  is thus

$$^i n = \frac{1}{\varepsilon Q} \left( \frac{d^iN}{dt} + {}^iN^i\lambda - {}^{i-1}N^{i-1}\lambda \right), \quad (\text{A2})$$

and the atmospheric activity  $^i a$  is

$$\begin{aligned} ^i a &= {}^i n^i\lambda = \frac{1}{\varepsilon Q} \left( \frac{d({}^iN^i\lambda)}{dt} + {}^i\lambda({}^iN^i\lambda - {}^{i-1}N^{i-1}\lambda) \right) \\ &= \frac{1}{\varepsilon Q} \left( \frac{d^iA}{dt} + {}^i\lambda({}^iA - {}^{i-1}A) \right). \end{aligned} \quad (\text{A3})$$

Due to its very short lifetime of  $^{214}\text{Po} \tau = 1/^{214}\text{Po} \lambda = 237 \mu\text{s}$ ,  $^{214}\text{Po}$  is not directly accumulated on the filter but generated through its accumulated precursor  $^{214}\text{Bi}$ . Also, at any instant there is radioactive equilibrium between  $^{214}\text{Po}$  and  $^{214}\text{Bi}$  activity in the atmosphere ( $^{214}\text{Po} a = ^{214}\text{Bi} a$ ) and on the filter ( $^{214}\text{Po} A = ^{214}\text{Bi} A$ ); thus

$$^{214}\text{Po} a = ^{214}\text{Bi} a = \frac{1}{\varepsilon Q} \left( \frac{d(^{214}\text{Bi} N^{214}\text{Bi} \lambda)}{dt} + ^{214}\text{Bi} \lambda \times (^{214}\text{Bi} N^{214}\text{Bi} \lambda - ^{214}\text{Pb} N^{214}\text{Pb} \lambda) \right). \quad (\text{A4})$$

Moreover, it can be shown that, even at an instantaneous change of the atmospheric  $^{222}\text{Rn}$  activity,  $^{214}\text{Pb} A$  and  $^{214}\text{Bi} A$  are almost at equilibrium (the maximum deviation is in the order of 18% and in most cases it is close to 5% (Stockburger, 1960)) so that we can substitute  $^{214}\text{Pb} N^{214}\text{Pb} \lambda$  by  $X^{214}\text{Bi} N^{214}\text{Bi} \lambda$  with

$$X = \frac{^{218}\text{Po} \tau + ^{214}\text{Pb} \tau}{^{218}\text{Po} \tau + ^{214}\text{Pb} \tau + ^{214}\text{Bi} \tau} = 0.6. \quad (\text{A5})$$

Therefore, substituting Eq. (A5) in Eq. (A4), we derive for the atmospheric  $^{214}\text{Bi}$  ( $=^{214}\text{Po}$ ) activity:

$$^{214}\text{Bi} a = \frac{p}{\varepsilon Q} \left( \frac{1}{p} \frac{d^{214}\text{Bi} A}{dt} + ^{214}\text{Bi} A \right) \quad (\text{A6})$$

with

$$\frac{1}{p} = ^{218}\text{Po} \tau + ^{214}\text{Pb} \tau + ^{214}\text{Bi} \tau$$

and

$$p = \frac{X}{^{214}\text{Bi} \lambda}.$$

The calculation of the atmospheric  $^{214}\text{Po}$  activity therefore needs the determination of the  $^{214}\text{Bi}$  filter activity  $^{214}\text{Bi} A$  ( $= ^{214}\text{Po} A$ ) as well as its rate of change at the time of the activity measurement.

### 6.3. Experimental determination of the $^{214}\text{Po}$ activity $^{214}\text{Po} A_\alpha$ on the filter

The accumulated  $\alpha$ -counts on the filter derived from  $^{222}\text{Rn}$  daughters ( $^{222}\text{Rn} M = ^{214}\text{Po} M + ^{218}\text{Po} M$ ) are calculated from the total measured  $\alpha$ -counts  $^{\text{total}} M$  on the filter according to Eq. (A7) (Fig. 7):

$$^{222}\text{Rn} M = ^{\text{total}} M - ^{\text{noise}} M - ^{220}\text{Rn} M \quad (\text{A7})$$

with  $^{220}\text{Rn} M$  being the  $^{220}\text{Rn}$  daughter counts ( $^{220}\text{Rn} M = ^{212}\text{Po} M + ^{212}\text{Bi} M$ ) on the filter.  $^{220}\text{Rn} M$  is

determined through the  $^{212}\text{Po}$  counts on the filter with  $\alpha_E > 7.7 \text{ MeV}$  using the following approximation:

$$^{220}\text{Rn} M = M(\alpha_E > 7.7 \text{ MeV}) c_{\text{tail}}(^{212}\text{Po}) \times r_{\text{branch}}(^{212}\text{Bi}; ^{212}\text{Po}) \quad (\text{A8})$$

The factor  $c_{\text{tail}}(^{212}\text{Po}) = 1/(0.778 \pm 0.015)$  accounts for  $^{212}\text{Po}$  counts overlapping with the  $^{214}\text{Po}$  peak (this factor has been determined empirically for various ratios of  $^{214}\text{Po}$  and  $^{212}\text{Po}$  activities). The factor  $r_{\text{branch}}(^{212}\text{Bi}; ^{212}\text{Po}) = 1/0.6407$  results from the branching ratio for  $^{212}\text{Bi}$  decay on the filter (35.93% by direct  $\alpha$ -decay and 64.07% via decay of  $^{212}\text{Po}$ ), which allows to calculate the total contribution of  $\alpha$ -particles from decay of  $^{212}\text{Bi}$ :

$$r_{\text{branch}} = \frac{^{212}\text{Bi} + ^{212}\text{Po}}{^{212}\text{Po}} = \frac{1}{0.6407} = 1.56.$$

Moreover, on the filter the  $\alpha$ -counts of both  $^{222}\text{Rn}$  daughters,  $^{214}\text{Po}$  ( $^{214}\text{Po} M$ ) and  $^{218}\text{Po}$  ( $^{218}\text{Po} M$ ), are measured, and it is necessary to also separate the  $^{218}\text{Po}$  counts  $^{218}\text{Po} M$  from the total  $^{222}\text{Rn}$  daughter counts  $^{222}\text{Rn} M$  to derive  $^{214}\text{Po} M$ . The low energy tailing of the  $\alpha$ -spectrum does, however, not allow spectroscopic separation of  $^{218}M_\alpha$ . Therefore, radioactive equilibrium is assumed between  $^{214}\text{Po}$  and  $^{218}\text{Po}$ , and the respective counts  $^{218}\text{Po} M = ^{214}\text{Po} M / 17.26 = 5.79\%$  are subtracted from the total  $^{222}\text{Rn}$  daughter counts on the filter  $^{222}\text{Rn} M$ . The  $^{214}\text{Po}$  counts on the filter are thus determined as:

$$^{214}\text{Po} M = 0.942 ^{222}\text{Rn} M \quad (\text{A9})$$

and the  $^{214}\text{Po}$  activity  $^{214}\text{Po} A$  on the filter is

$$^{214}\text{Po} A = \frac{^{214}\text{Po} M}{\Delta T} \quad (\text{A10})$$

with  $\Delta T$  being the acquisition time. The mean  $^{214}\text{Po} A$  filter activities are determined from the spectra in each measurement interval (integrated over 30 min), additionally taking into account the relative solid angle  $\Omega$  of the detector:

$${}^{214}\text{Po} A = \frac{1}{\Omega} \frac{0.942(\text{total } M - \text{noise } M - M(\alpha_E > 7.7 \text{ MeV}))c_{\text{tail}} r_{\text{branch}}}{\Delta T}. \quad (\text{A11})$$

This solid angle has been determined from the geometry of the filter holder, i.e. the active surface of the detector ( $R_D = 1.693$  cm), the aerosol-loaded surface of the filter ( $R_F = 1.704$  cm) and the distance between the filter and the detector (filter and detector surfaces are mounted in parallel). For the actual distance between filter and the detector in the Heidelberg monitor of  $d = 0.565$  cm the solid angle was calculated as 0.2650 (Cuntz, 1997). For intercomparison of the monitors the combined individual solid angle and detector efficiency are checked through measurement of an  $\alpha$ -source ( ${}^{241}\text{Am}$ ,  $\alpha_E = 5.49$  MeV) with a similar geometry as an aerosol filter. This measurement is regularly repeated to check the efficiency of the  $\alpha$ -detector.

#### 6.4 Intercomparison experiments

Two intercomparison experiments have been conducted with the Laboratoire des Sciences du Climat

et de l'Environnement, Gif-sur-Yvette, France, at Gif-sur-Yvette close to Paris in April 1998 and at Mace Head, Ireland ( $53^\circ\text{N}$ ,  $10^\circ\text{W}$ , 5 m a.s.l.), in October 2000. The French measurement system also determines  ${}^{222}\text{Rn}$  via its short-lived daughters (Polian et al., 1986). For a wide range of ambient activities between 0.1 and  $10 \text{ Bq m}^{-3}$ , both experiments yielded very good agreement between the two measurement systems of better than  $\pm 10\%$ . Another intercomparison experiment was performed with the Bundesamt für Strahlenschutz, Institut für Atmosphärische Radioaktivität, Freiburg, Germany, comparing their  ${}^{222}\text{Rn}$  measurements derived from  $\alpha$ - and  $\beta$ -activity counting of  ${}^{222}\text{Rn}$  decay products accumulated on a static filter (Stockburger 1960) with those of our radon monitor at the Schauinsland station in the Black Forest ( $48^\circ\text{N}$ ,  $8^\circ\text{E}$ , 1205 m a.s.l.) during two weeks in March 1997. Ambient activities varied between 0.5 and  $7 \text{ Bq m}^{-3}$ . Within a standard deviation of  $\pm 5\%$ , no significant differences were observed between the two measurement systems (Cuntz, 1997).

#### REFERENCES

- Biraud, S., Ciais, P., Ramonet, M., Simmons, P., Kazan, V., Monfray, P., O'Doherty, S., Spain, G. and Jennings, S. J. 2000. European greenhouse gas emissions estimated from continuous atmospheric measurements and Radon-222 at Mace Head, Ireland. *J. Geophys. Res.* **105**, 1351–1366.
- Chevillard, A., Ciais, P., Karstens, U., Heimann, M., Schmidt, M., Levin, I., Jacob, D., Podzun, R., Kazan, V., Sartorius, H. and Weingartner, E. 2002. Transport of  ${}^{222}\text{Rn}$  using the regional model REMO: A detailed comparison with measurements over Europe. *Tellus* **54B**, this issue.
- Cuntz, M. 1997. The Heidelberg  ${}^{222}\text{Rn}$  monitor: Calibration, optimisation, application. Thesis, Institut für Umweltphysik, University of Heidelberg, Germany (in German).
- Dörr, H., Kromer, B., Levin, I., Münnich, K. O. and Volpp, H. J. 1983.  $\text{CO}_2$  and radon-222 as tracers for atmospheric transport. *J. Geophys. Res.* **88**, 1309–1313.
- Dörr, H. and Münnich, K. O. 1990.  ${}^{222}\text{Rn}$  flux and soil air concentration profiles in West Germany. Soil  ${}^{222}\text{Rn}$  as tracer for gas transport in the unsaturated soil zone. *Tellus* **42B**, 20–28.
- Fischer, K. 1976. A slow-pulse ionization chamber for the measurement of radon in air. Thesis, Institut für Umweltphysik, University of Heidelberg, Germany (in German).
- Jacobi, W. and André, K. 1963. The vertical distribution of  ${}^{222}\text{Rn}$ ,  ${}^{220}\text{Rn}$  and their decay products in the atmosphere. *J. Geophys. Res.* **68**, 3799–3814.
- Kuhlmann, A. J., Worthy, D., Trivett, N. B. A. and Levin, I. 1998. Methane emissions from a wetland region within the Hudson Bay Lowland: an atmospheric approach. *J. Geophys. Res.* **103**, 16 009–16 016.
- Langendörfer, U., Cuntz, M., Ciais, P., Peylin, P., Bariac, T., Milukova, I., Kolle, O., Naegler, T. and Levin, I. 2002. Modelling of biospheric  $\text{CO}_2$  gross fluxes via oxygen isotopes: a  ${}^{222}\text{Rn}$ -calibrated box model approach. *Tellus* **54B**, this issue.
- Levin, I. 1984. Atmospheric  $\text{CO}_2$ , sources and sinks on the European continent. PhD-Thesis, University of Heidelberg, Germany (in German).
- Levin, I., Schuchard, J., Kromer, B. and Münnich, K. O. 1989. The continental European Suess effect. *Radiocarbon* **31**, 431–440.
- Levin, I., Glatzel-Mattheier, H., Marik, T., Cuntz, M., Schmidt, M. and Worthy, D. E. 1999. Verification of German methane emission inventories and their recent changes based on atmospheric observations. *J. Geophys. Res.* **104**, 3447–3456.
- Nazaroff, W. N. 1992. Radon transport from soil to air. *Rev. Geophys.* **30**, 137–160.

- Polian, G., Lambert, G., Ardouin, B. and Jegou, A. 1996. Long-range transport of continental radon in Subantarctic and Antarctic areas. *Tellus* **38B**, 178–189.
- Porstendörfer, J., Butterweck, G. and Reineking, A. 1991. Diurnal variation of the concentrations of radon and its short-lived daughters in the atmosphere near ground. *Atmos. Environ.* **25**, 709–713.
- Rebmann, C. and Kolle, O. 2000. *Documentation of EDDY software*. Max Planck Institut für Biogeochemie, Jena, Germany.
- Reineking, A. and Porstendörfer, J. 1990. Unattached fraction of short-lived Rn decay products in indoor and outdoor environments: an improved single-screen method and results. *Health Phys.* **58**, 715–727.
- Roether, W. and Kromer, B. 1978. Field determination of air-sea gas exchange by continuous measurement of radon-222. *Pageoph.* **116**, 476–485.
- Schery, S. D., Gaeddert, D. H. and Wilkening, M. H. 1984. Factors effecting exhalation of radon from gravelly, sandy loam. *J. Geophys. Res.* **89**, 7299–7309.
- Schery, S. D. and Wasiolek, P. T. 1993. A two-particle-size model and measurements of radon progeny near the Earth's surface. *J. Geophys. Res.* **98**, 22 915–22 923.
- Schmidt, M., Glatzel-Mattheier, H., Sartorius, H., Worthy, D. E. and Levin, I. 2001. Western European  $\text{N}_2\text{O}$  emissions – a top down approach based on atmospheric observations. *J. Geophys. Res.* **106**, 5507–5516.
- Schuepp, P. H., Leclerc, M. Y., MacPherson, J. I. and Desjardins, R. L. 2000. Footprint prediction of scalar fluxes from analytical solutions of the diffusion equation. *Boundary-Layer Meteorol.* **50**, 355–373.
- Schüßler, W. 1996. *Effective parameters to determine gas-exchange between soil and atmosphere*. PhD Thesis, University of Heidelberg, Germany (in German).
- Schumann, G. 1956. Untersuchung der Radioaktivität der Atmosphäre mit der Filtermethode. *Archiv für Meteorol., Geophys. Bioklimatol. Ser. A* **9**, 205–223.
- Stockburger, H. 1960. *Continuous registration of the radon-, thorium-B and decay product activity of atmospheric air*. PhD Thesis, University of Freiburg, Germany (in German).
- Verclas, S. 1994. *Set-up and test of a monitor to measure the atmospheric  $^{222}\text{Rn}$  daughter activity, and first measurements*. Thesis, Institut für Umweltp Physik, University of Heidelberg, Germany (in German).
- Volpp, H.-J. 1984. *Investigation of large scale atmospheric transport in Central Europe with radon-222*. PhD Thesis, University of Heidelberg, Germany (in German).
- Wilkening, M. H. and Clements, W. E. 1975. Radon-222 from the ocean surface. *J. Geophys. Res.* **80**, 3828–3830.
- Wilson, S. R., Dick, A. L., Fraser, P. J. and Whittlestone, S. 1997. Nitrous oxide flux estimates for south-eastern Australia. *J. Atmos. Chem.* **26**, 169–188.
- Whittlestone, S. 1990. Radon daughter disequilibria in the lower marine boundary layer. *J. Atmos. Chem.* **11**, 27–42.